Mendeleev Communications

Mendeleev Commun., 2025, **35**, 475–477

Synthesis of hybrid Ta_2O_5@PDA/Au nanocomposites

Ekaterina D. Koshevaya,*[a] Elena M. Shishmakova,[b] Alexandr V. Belousov,[a] Vladimir N. Morozov,[c] Maria A. Kolyvanova[a,c] and Olga V. Dement'eva[b]

[a] *Burnasyan Federal Medical Biophysical Center of Federal Medical Biological Agency, 123182 Moscow, Russian Federation. Fax: +7 901 330 1558; e-mail: katiakosh@gmail.com*

[b] *A. N. Frumkin Institute of Physical Chemistry and Electrochemistry, Russian Academy of Sciences, 119071 Moscow, Russian Federation*

[c] *N. M. Emanuel Institute of Biochemical Physics, Russian Academy of Sciences, 119334 Moscow, Russian Federation*

DOI: 10.71267/mencom.7672

Hybrid Ta_2O_5/Au nanoparticles (NPs) were synthesized by *in situ* radiolytic reduction of Au ions in a tantalum oxide hydrosol. For efficient Au binding, Ta_2O_5 NPs were preliminarily modified with a polydopamine (PDA) layer. This one-pot approach allows the monodispersed Au NPs to be directly anchored on the Ta_2O_5@PDA surface, which compares favourably with the conventional multi-stage method for synthesizing such structures.

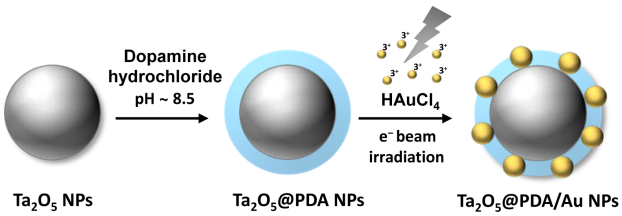

Keywords: tantalum oxide, gold, hybrid nanoparticles, polydopamine coating, radiation synthesis.

Hybrid metal oxide/metal nanoparticles (NPs) are increasingly recognized for their potential in various practical applications. For example, Au[1,2] and Ta_2O_5[3] NPs are showing promise for use as components of such hybrids in biomedicine. As biocompatible and non-toxic materials, they show great potential for the development of new radiosensitizers and contrast agents.[4–7] It is noteworthy that at the same time, they can also serve as efficient catalysts.[8] Thus, their combination and, specifically, the modification of the Ta_2O_5 surface with Au NPs may open up a possibility of obtaining complex nanostructures with new functional properties.

However, tantalum oxide is known to be a highly inert compound, which makes difficult its direct modification. To facilitate the binding of gold to tantalum oxide, we propose here the coating of Ta_2O_5 NPs with polydopamine (PDA). This biopolymer contains a variety of functional groups, such as catechol, amine and imine, allowing it to form strong bonds with metals.[9,10]

In general, hybrid materials can be obtained by mixing individually synthesized components. However, the development of new strategies for the *in situ* synthesis of hybrids is important from both economic and environmental points of view. Thus, in the present work, we propose the formation of Ta_2O_5@PDA/Au hybrids by radiolytic reduction of Au ions in the dispersion medium of the Ta_2O_5@PDA hydrosol. In this method, the reducing agents such as solvated electrons (e^-_{aq}) and hydrogen radicals ($H^\bullet$) are generated directly during the radiolysis of water, which minimizes the quantity of by-products and contaminants. The radiation-induced synthesis is emerging as a highly efficient green alternative to chemical methods for synthesizing metal nanoclusters and/or NPs.[11–13] The radiation approach to synthesis of hybrid structures containing gold NPs has been investigated,[14] but this is the first time it has been applied to tantalum oxide NPs.

At the first step, a hydrosol of tantalum oxide NPs was prepared using a solvothermal synthesis method, followed by the replacement of the alcohol dispersion medium with water[15,†] (see Online Supplementary Materials, Section S1). According to the transmission electron microscopy (TEM) data, the synthesized NPs had a spherical shape, an amorphous structure and an average size of 30 nm. To coat the NPs with a PDA shell, the hydrosol of Ta_2O_5 was mixed with a dopamine hydrochloride solution (Section S2, Online Supplementary Materials). Polymerization of dopamine took place at alkaline pH. The TEM image and the corresponding size histogram of the Ta_2O_5@PDA NPs is shown in Figure 1(*a*). As is seen, the surface of the oxide NPs became quite uneven after the deposition of PDA. According to statistical analysis, the average size of NPs increased to 34.6 ± 11.5 nm. The presence of functional groups on the NP surface before and after modification was explored by FTIR spectroscopy (Figure 2). The infrared spectrum of the bare NPs contains a broad peak (500–1000 cm^{-1}) attributed to tantalum oxide, as well as the peaks of O–H stretching vibrations (3400 cm^{-1}) and H_2O deformation vibrations (1630 cm^{-1}). After coating with PDA, a series of new peaks appeared in the range of 1250–1550 cm^{-1}, clearly indicating the successful attachment of PDA molecules to the NP surface. The peak at 1490 cm^{-1} may be ascribed to the C=N and C=C vibrations[16] or NH_2 scissoring vibrations of indole structures,[17] while the peak at 1270 cm^{-1} is attributed to the C–O bond of catechol.[16] After decoration of Ta_2O_5@PDA cores with Au NPs, the peaks at 1490 cm^{-1} and 1270 cm^{-1} practically disappeared. This suggests that the coordination of Au occurred through the amino and catechol groups.[7]

In this work, the two approaches to synthesis of Ta_2O_5@PDA/Au hybrid NPs were compared. The first one consisted of mixing the dispersion of Ta_2O_5@PDA particles with a preliminary synthesized gold hydrosol. The second one, in turn, involved the

† For details on the synthetic procedures of Ta_2O_5 (Section S1), Ta_2O_5@PDA (Section S2), Au (Section S3) and Ta_2O_5@PDA/Au (Section S4) NPs, as well as on characterization methods (Section S5), please refer to the Online Supplementary Materials.

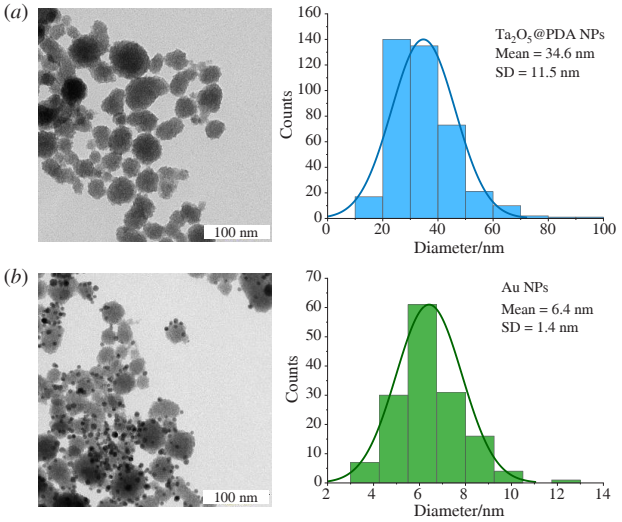

Figure 1 (*a*) TEM image and size distribution histogram of Ta_2O_5@PDA NPs and (*b*) TEM image of Ta_2O_5@PDA/Au NPs produced by mixing and size distribution histogram of Au NPs synthesized by irradiation at 5 kGy.

radiation-induced reduction of gold ions directly in the Ta_2O_5@PDA dispersion. The Au NPs, which were further used to obtain the Ta_2O_5@PDA/Au composite by mixing, were also produced by radiation-induced reduction of the metal ions in water (Section S3). The obtained Au NP sol (Figure 3) exhibited a surface plasmon resonance (SPR) band close to 516 nm. The particle size calculated using the method described by Haiss *et al.*[18] was ~6.5 nm.

The TEM image and size distribution histogram of Ta_2O_5@PDA/Au hybrid NPs, obtained by mixing (Section S4), are presented in Figure 1(*b*). The Au NPs were found to be randomly distributed over the oxide surface. It is noteworthy that all detected Au NPs were firmly attached to the oxide; no free Au NPs were found. According to statistical analysis, the mean size of Au NPs was 6.4 ± 1.4 nm.

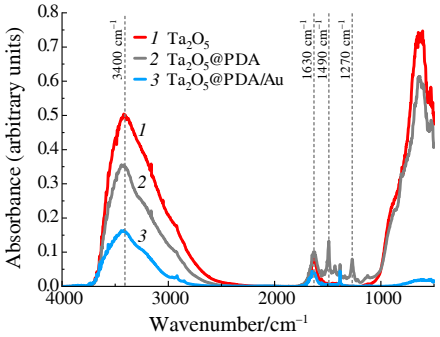

Figure 2 FTIR spectra of (*1*) Ta_2O_5 (red), (*2*) Ta_2O_5@PDA (grey) and (*3*) Ta_2O_5@PDA/Au (blue) NPs.

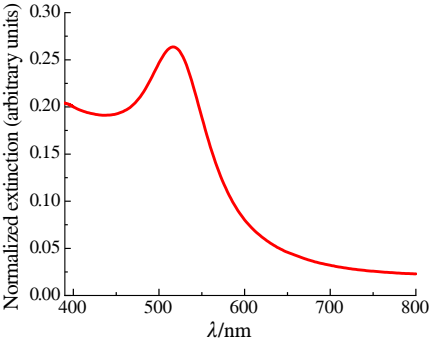

Figure 3 Extinction spectrum of the synthesized Au NPs in water.

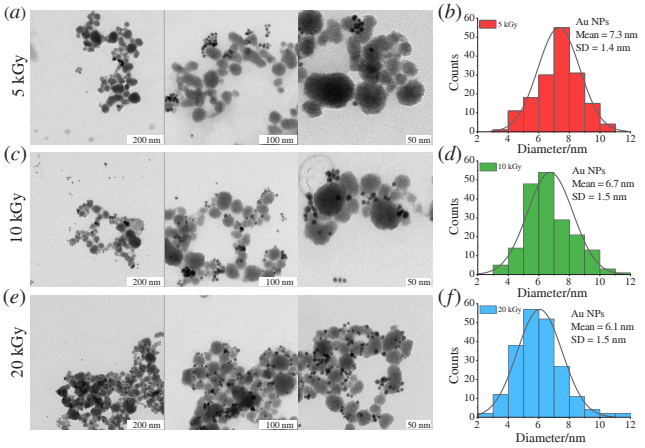

Figure 4 TEM images of hybrid Ta_2O_5@PDA/Au NPs and corresponding size distribution histograms of Au NPs synthesized through irradiation at (*a*),(*b*) 5 kGy, (*c*),(*d*) 10 kGy and (*e*),(*f*) 20 kGy.

The TEM images and size distribution histograms of Ta_2O_5@PDA/Au hybrid NPs obtained by radiolytic approach (Section S4) are presented in Figure 4. The images show sols before the washing procedure, which allows a more complete assessment of unbound particles. It is evident that irradiation of the $HAuCl_4$ solution in the presence of Ta_2O_5@PDA NPs led to the formation of gold Au NPs, exhibiting a dose-dependent effect. At 5 kGy, a non-homogeneous distribution of Au NPs was observed, with only a small portion of the tantalum oxide NPs covered [(Figure 4(*a*)]. Small clusters and unbonded Au particles could be seen. Increasing the irradiation dose to 10 kGy resulted in a more uniform distribution, though a significant amount of unbonded Au NPs were observed [Figure 4(*c*)]. The use of 20 kGy promotes more homogeneous coverage of Ta_2O_5 with Au NPs, and the number of unbonded particles was significantly lower [Figure 4(*e*)]. Furthermore, the mean size of Au NPs decreased with increasing dose, being equal to 7.3 ± 1.4 nm at 5 kGy and 6.1 ± 1.5 nm at 20 kGy [Figures 4(*b*),(*d*),(*f*)]. The more detailed exploration of the features of this process and establishing of the relationships between irradiation conditions and structure of the obtained hybrid system will be the subject of the further works.

Figure 5 shows the extinction spectra of the obtained Ta_2O_5@PDA/Au hydrosols. The SPR maxima were observed at a wavelength of 522 nm for all sols after 3 cycles of centrifugation and redispersion.

In conclusion, the Ta_2O_5@PDA/Au hybrid NPs were synthesized by *in situ* radiolitic reduction of the Au precursor in the presence of tantalum oxide NPs. Efficient Au NP binding was provided by the usage of the PDA coating. The results indicate that the mean size of Au NPs decreases at higher irradiation doses, showing a dose-dependent effect on

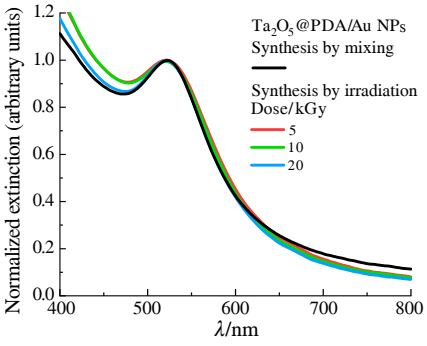

Figure 5 Extinction spectra of Ta_2O_5@PDA/Au NPs obtained by mixing or electron irradiation at 5, 10 and 20 kGy. The spectra were normalized against the intensities of the SPR peak.

Ta_2O_5@PDA coverage with Au NPs. It was shown that the hybrid particles produced by *in situ* radiolytic synthesis at 20 kGy had characteristics very close to those of the system obtained by mixing the PDA-coated oxide with the preliminary synthesized Au NPs. Both hybrids were characterized by the Ta_2O_5@PDA core of ~35 nm in size and the surface bound Au NPs of ~6 nm in size with narrow size distributions. However, the presented *in situ* approach reduces the number of synthesis steps.

This work demonstrates the potential of radiolytic methods for synthesizing hybrid nanostructures with tailored properties. Considering the ability of PDA and Au NPs to bind to various drugs and biomolecules,[19,20,21] it can be expected that their localization on tantalum oxide will allow the development of novel platforms for targeted drug delivery and chemoradiotherapy.

This work was supported by the Russian Science Foundation (grant no. 24-23-00510).

Online Supplementary Materials

Supplementary data associated with this article can be found in the online version at doi: 10.71267/mencom.7672.

References

1 N. K. Ivanova, E. A. Karpushkin, L. I. Lopatina and V. G. Sergeyev, *Mendeleev Commun.*, 2023, **33**, 346; https://doi.org/10.1016/j.mencom.2023.04.016.
2 A. A. Vodyashkin, M. G. H. Rizk, P. Kezimana, A. A. Kirichuk and Y. M. Stanishevskiy, *ChemEngineering*, 2021, **5**, 69; https://doi.org/10.3390/chemengineering5040069.
3 E. Koshevaya, E. Krivoshapkina and P. Krivoshapkin, *J. Mater. Chem. B*, 2021, **9**, 5008; https://doi.org/10.1039/D1TB00570G.
4 M. A. Kolyvanova, A. V. Belousov, G. A. Krusanov, A. K. Isagulieva, K. V. Morozov, M. E. Kartseva, M. H. Salpagarov, P. V. Krivoshapkin, O. V. Dement'eva, V. M. Rudoy and V. N. Morozov, *Int. J. Mol. Sci.*, 2021, **22**, 6030; https://doi.org/10.3390/ijms22116030.
5 E. Koshevaya, D. Nazarovskaia, M. Simakov, A. Belousov, V. Morozov, E. Gandalipov, E. Krivoshapkina and P. Krivoshapkin, *J. Mater. Chem. B*, 2020, **8**, 8337; https://doi.org/10.1039/d0tb01204a.
6 A. Alhussan, N. Jackson, R. Calisin, J. Morgan, W. Beckham and D. B. Chithrani, *Int. J. Mol. Sci.*, 2023, **24**, 12523; https://doi.org/10.3390/ijms241512523.
7 C. Ji, M. Zhao, C. Wang, R. Liu, S. Zhu, X. Dong, C. Su and Z. Gu, *ACS Nano*, 2022, **16**, 9428; https://doi.org/10.1021/acsnano.2c02314.
8 M. Lin, C. Mochizuki, B. An, Y. Inomata, T. Ishida, M. Haruta and T. Murayama, *ACS Catal.*, 2020, **10**, 9328; https://doi.org/10.1021/acscatal.0c01966.
9 L. Wang, K. Song, C. Jiang, S. Liu, S. Huang, H. Yang, X. Li and F. Zhao, *Adv. Healthcare Mater.*, 2024, **13**, 2401451; https://doi.org/10.1002/adhm.202401451.
10 Y. S. Lee, J. Y. Bae, H. Y. Koo, Y. B. Lee and W. S. Choi, *Sci. Rep.*, 2016, **6**, 22650; https://doi.org/10.1038/srep22650.
11 S. M. Ghoreishian, S.-M. Kang, G. S. R. Raju, M. Norouzi, S.-C. Jang, H. J. Yun, S. T. Lim, Y.-K. Han, C. Roh and Y. S. Huh, *Chem. Eng. J.*, 2019, **360**, 1390; https://doi.org/10.1016/j.cej.2018.10.164.
12 A. A. Zharikov, E. A. Zezina, A. V. Sybachin, A. L. Vasiliev, A. I. Emel'yanov, A. S. Pozdnyakov, V. I. Feldman and A. A. Zezin, *Radiat. Phys. Chem.*, 2024, **224**, 112059; https://doi.org/10.1016/j.radphyschem.2024.112059.
13 D. A. Migulin, J. V. Rozanova, A. A. Zharikov, V. I. Feldman, O. V. Emelyanova and A. A. Zezin, *J. Photochem. Photobiol., A*, 2025, **458**, 115980; https://doi.org/10.1016/j.jphotochem.2024.115980.
14 M. C. Molina Higgins, D. M. Clifford and J. V. Rojas, *Appl. Surf. Sci.*, 2018, **427A**, 702; https://doi.org/10.1016/j.apsusc.2017.08.094.
15 E. Koshevaya, V. Mikhaylov, P. Sitnikov, E. Krivoshapkina and P. Krivoshapkin, *Surf. Interfaces*, 2022, **29**, 101713; https://doi.org/10.1016/j.surfin.2021.101713.
16 H. Luo, C. Gu, W. Zheng, F. Dai, X. Wang and Z. Zheng, *RSC Adv.*, 2015, **5**, 13470; https://doi.org/10.1039/c4ra16469e.
17 C.-C. Ho and S.-J. Ding, *J. Mater. Sci.: Mater. Med.*, 2013, **24**, 2381; https://doi.org/10.1007/s10856-013-4994-2.
18 W. Haiss, N. T. K. Thanh, J. Aveyard and D. G. Fernig, *Anal. Chem.*, 2007, **79**, 4215; https://doi.org/10.1021/ac0702084.
19 M. Li, X. Zhang, S. Li, X. Shao, H. Chen, L. Lv and X. Huang, *RSC Adv.*, 2021, **11**, 18198; https://doi.org/10.1039/D1RA02116H.
20 G. Fitzgerald, D. Low, L. Morgan, C. Hilt, M. Benford, C. Akers, S. Hornback, J. Z. Hilt and D. Scott, *J. Pharm. Sci.*, 2023, **112**, 1064; https://doi.org/10.1016/j.xphs.2022.12.001.
21 S. Geng, Q. Feng, C. Wang, Y. Li, J. Qin, M. Hou, J. Zhou, X. Pan, F. Xu, B. Fang, K. Wang and Z. Yu, *J. Nanobiotechnol.*, 2023, **21**, 338; https://doi.org/10.1186/s12951-023-02072-1.

Received: 1st November 2024; Com. 24/7672